tvst

Article

Safety Evaluation of Photoacoustic Tomography System for Intraocular Tumors

Guan Xu[1,2], Naheed Khan[1], Ahmed Almazroa[1,3], Mercy Pawar[1], Cagri Besirli[1], Yannis M. Paulus[1,2], Xueding Wang[2,4], and Hakan Demirci[1]

[1] Department of Ophthalmology and Visual Sciences, University of Michigan Medical School, Ann Arbor, MI, USA
[2] Department of Biomedical Engineering, University of Michigan Medical School, Ann Arbor, MI, USA
[3] King Abdullah International Medical Research Center/King Saud bin, Abdulaziz University for Health Science, Saudi Arabia
[4] Department of Radiology, University of Michigan Medical School, Ann Arbor, MI, USA

Correspondence: Guan Xu, Department of Ophthalmology and Visual Sciences, University of Michigan Medical School, 1515 E. Medical Center Drive, Ann Arbor, MI 48109, USA.
e-mail: guanx@umich.edu
Hakan Demirci, Department of Ophthalmology and Visual Sciences, University of Michigan Medical School, 1515 E. Medical Center Drive, Ann Arbor, MI 48109, USA.
e-mail: hdemirci@umich.edu

Received: September 8, 2021
Accepted: January 13, 2022
Published: March 28, 2022

Keywords: photoacoustic tomography; intraocular tumor; laser toxicity

Citation: Xu G, Khan N, Almazroa A, Pawar M, Besirli C, Paulus YM, Wang X, Demirci H. Safety evaluation of photoacoustic tomography system for intraocular tumors. Transl Vis Sci Technol. 2022;11(3):30, https://doi.org/10.1167/tvst.11.3.30

Purpose: Photoacoustic tomography (PAT) has demonstrated the ability to characterize molecular components and architectural heterogeneities of intraocular tumors in enucleated human globes and in animals in vivo. Although laser safety levels have been established for illumination through the cornea, the safety limit for PAT illumination through the sclera has not been investigated. The purpose of this study is to examine if the energy level used in intraocular PAT results in ocular damage.

Methods: Rabbit eyes were exposed to pulsed laser illumination at 20 mJ/cm^2 at the scleral surface. Eyes were examined at 1, 7, and 28 days after the laser exposure. Examination procedures included white light and fluorescence fundus imaging, optical coherence tomography (OCT), electroretinography (ERG), and histology with hematoxylin and eosin (H&E) staining as well as terminal deoxynucleotidyl transferase-mediated deoxyuridine triphosphate nick-end labeling (TUNEL staining).

Results: Fundus imaging and OCT of rabbit eyes at 1, 7, and 28 days following exposure of the laser illumination of the PAT system did not reveal any damage to the retinal structures. ERG showed no significant difference between the experimental and control eyes. Similarly, H&E histology did not show abnormalities in either the scleral tissue where the laser illumination was delivered or in the retinal layers. No sign of apoptosis in the layers of the retina, choroid, or optic nerve was found on TUNEL staining.

Conclusions: Similar to the application of PAT to other organs, the proposed laser illumination energy level at 20 mJ/cm^2 does not impose detectable harm to the ocular tissue.

Translational Relevance: This study addresses illumination safety issues for PAT.

Introduction

Photoacoustic tomography (PAT) has demonstrated promise in assessing the unique molecular and architectural features of ocular tumors.[1,2] In contrast to photoacoustic microscopy,[3–5] which has been used to evaluate vasculature in the posterior segment of the eye, PAT generates signals with wide-field laser illumination through the anterior segment of the sclera and captures the signals with an ultrasound transducer array.[6] Such a data acquisition scheme provides a unique advantage of high frame rate imaging and deep penetration for assessing large tissue volume while avoiding the focusing effect of the lens to the light beam. Our previous study with PAT has demonstrated its ability to delineate intraocular tumors and differentiate uveal melanoma and retinoblastoma in enucleated human eyes.[1,2] PAT, therefore, could be a potential tool complementary to other

diagnostic modalities for characterizing intraocular tumors.

Pioneering studies have investigated ocular toxicity of wide-field or weakly focused optical energy. Lund et al.[7] investigated the energy threshold to damage the retina in monkeys using a 7 ns pulse laser at 10 Hz repetition rate and showed that the energy threshold to cause the retinal damage was 33.9 mJ/cm^2 for 100 continuous exposures at 532 nm. Yumita et al.[8] have reported a damage energy threshold of 296.3 µJ at 532 nm with an 80 µm spot size at the retina, which is equivalent to 5.9 J/cm^2. One limitation of these studies is that the illuminations are all at single wavelength instead of multiple wavelengths. In addition, all of these studies, as well as the safety regulations established by the American National Standards Institute (ANSI), focused on the optical density at the retina. A study on the safe optical density at the sclera will be of great interest for clinical translation of PAT.

The sclera plays a critical role in maintaining the ocular structure, attenuating optical energy, and protecting the posterior segment of the eye from photothermal damage. The optical properties of the sclera have been studied previously. Vogel et al.[9] evaluated the total transmission, absorption, and reflection at different laser wavelengths. They found that scleral transmission was 6% at 442 nm wavelength, but it increased to 53% at 1064 nm when non-contact illumination was used. When the illumination was delivered through an optical fiber with the tip in contact with the sclera, scleral transmission increased by a factor of 3.5 at 442 nm, 2.0 at 804 nm, and by 1.5 at 1064 nm. With firm pressure, the scleral transmission increased even more. In another study, Smith and Stein[10] found that laser transmission through the human sclera was 31% $\pm$ 9.1 at 694 nm and 45% $\pm$ 11.2 at 1060 nm. Transmission through the combined human sclera, choroid, and retina layers were 10.4% $\pm$ 4.5 at 694 nm and 36.5% $\pm$ 8.3 at 1060 nm. Besides absorption, the scattering effect of the sclera also reduces the optical density at the retina by substantially weakening the directivity of the illumination. Bashkatov et al.[11] reported that the reduced scattering coefficient (μ_s') of scleral tissue is at least 4.5 mm^{-1} in the 700–1000 nm range. Considering that the thickness of sclera in the anterior segment is approximately 500 µm, only 10.5% (=exp[$-\mu_s'$d] = exp[-4.5×0.5]) of the optical energy will maintain the original directivity when propagated through the sclera. The rest of the energy will travel in random directions and illuminate a large area of the retina.

In spite of the attenuating factors of the sclera, light emitting diode (LED) based PAT can achieve real time imaging with desirable signal-to-noise ratio by averaging signals generated by hundreds of pulsed illuminations at the repetition rate of KHz. The energy level of such illumination falls into the ocular safety range established by the International Electrotechnical Commission (IEC) 62471.[12] However, LED light sources are not wavelength tunable and, therefore, have limited the potential of extracting the optical spectroscopic information within lesions for differential diagnosis.

As an alternative, an optical parametric oscillator (OPO) pumped by a Nd:YAG laser possesses high output energy and wide tunability. The high energy level also allows for deeper penetration and quantitative evaluation of the microscopic architecture within tumors.[1] With output from an OPO laser at multiple wavelengths, we were able to extract tissue components using spectroscopic information within intraocular tumors ex vivo.[1]

This study investigated the ocular safety of the wide-field illumination provided by the OPO laser in our PAT system[1] in rabbit eyes. Experimental and control eyes were examined with imaging modalities, including white light and fluorescence fundus photography and optical coherence tomography (OCT). Retinal function was evaluated by electroretinography (ERG). Potential damage to the sclera, retina, and choroid was also examined by histopathology.

Methods and Materials

Animals

The animal experiment protocol in this study has been approved by the Institutional Animal Care and Use Committee (IACUC) at the University of Michigan. A total of 12 normal New Zealand white rabbits of both genders with body weight of 2 to 2.5 kg were used. During all procedures, the rabbits were anesthetized with a mixture of ketamine (40 mg/kg) and xylazine (4 mg/kg) by intramuscular injection. For each animal, only the right eye was exposed to laser illumination. The left eye was covered by surgical tape during the laser exposure and used as control. The rabbits were divided into three groups with four subjects each. The 3 groups were examined at 1, 7, and 28 days after the wide-field laser illumination. Before all examinations, pupillary dilation was performed with 0.05 mL of 1% tropicamide and 0.05 mL of 2.5% phenylephrine hydrochloride. Topical tetracaine 0.5% was instilled in the treated eyes before imaging. During the experiments, eyewash (Altaire Pharmaceuticals, Inc., Aquebogue, NY) was applied to rabbit cornea every 2 minutes to prevent corneal surface keratopathy. Vitals, such as heart rate, respiratory rate, and rectal temperature, as well as mucous membrane color were monitored and recorded every 15 minutes.

Wide-Field Laser Illumination Setup

The optical illumination was generated by an OPO laser (Vibrant; OPOTEK, Carlsbad, CA) with pulse duration of 8 ns. Illumination from the wavelengths of 700 nm to 950 nm with steps of 50 nm was used. To simulate the signal averaging at the imaging procedure, illumination at each wavelength was delivered 10 times at a repetition rate of 10 Hz.

The laser illumination was delivered to the sclera using a fiber optic bundle with a radius of 3.2 mm and numerical aperture of 0.39. The fiber optic bundle was over the equator of the right eye sclera at 12 clock meridians, similar to our previous study. The cornea and limbus were avoided. The optical energy density at the emission end of the fiber bundle (i.e. the sclera surface), was maintained at 20 mJ/cm^2, which is the safety limit established by the American National Standards Institute on skin surface and tentatively used in our previous imaging protocol.[1]

As reported in previous studies, the average axial length[13] and the retinal area[14] of rabbit globes are 18.1 mm and 520 mm^2, respectively. Therefore, the illumination delivered by the fiber optic bundle, without the scattering effect of the sclera, is 371 mm^2 ($\pi r^2 = \pi \times (18.1\text{ mm} \times \tan[\arcsin 0.39] + 3.2\text{ mm})^2$), which is 71% of the total retinal surface area. In addition, similar to the estimate with human sclera in introduction, only 41% (=exp[$-\mu_s'$d] = exp[-4.5×0.2]) optical energy delivered through the rabbit sclera maintained its directivity. Therefore, 59% of the optical energy propagated through sclera will be scattered across 71% of the retinal area as calculated above, leading to a sufficiently large exposed area for assessing retinal damage with ERG.

Optical Coherence Tomography

Optical coherence tomography (OCT) has been frequently used in the imaging and evaluation of the retinal and choroidal layers of the eye. We used a commercial spectral-domain OCT system (Ganymede-II-HR; Thorlabs, Newton, NJ) to examine the integrity of both retinal and choroidal layers in the superior quadrant of the fundus and surrounding area where the wide-field laser illumination was applied. Each image was generated in less than 1 second.

White Light and Fluorescence Enhanced Fundus Photography

Fundus photography has the capability to assess anatomic features and vascular integrity at the posterior section of the eye. A fundus camera (TRC 50EX; Topcon Corporation, Tokyo, Japan) with wide-field and fluorescence contrast enhancement with Indocyanine Green (ICG) was used to identify anatomic features and changes to the vasculature of the eye.

Electroretinography

Full-field ERGs were performed with an LKC UTAS 3000 electrophysiology system (LKC Technologies, Gaithersburg, MD) with a Ganzfeld configuration. The rabbits were dark-adapted overnight and anesthetized by intraperitoneal injection of ketamine 100 mg/kg and xylazine 10 mg/kg. Following pupil dilation with 0.5% tropicamide topical anesthesia and application of 0.5% proparacaine and 2% methylcellulose to maintain corneal hydration, ERGs were recorded with bipolar contact lens electrodes (Mayo Corporation, Aichi, Japan). The ground needle electrode was placed subcutaneously on the scruff. Responses were amplified at a gain of 2500, band pass filtered at 0.3 to 500 Hz and were digitized at a rate of 2000 Hz. Animals were kept on a warming plate during the entire ERG procedure to maintain the body temperature at 37°C. Dark-adapted rod isolated ERG responses were recorded at 0.01 cd.s/m^2 white light (6500 K) flashes presented at an interstimulus interval of 3 seconds and the combined rod-cone response was recorded with 3.0 cd.s/m^2 flashes at intervals of 30 seconds. Averages ranged from 10 trials for dim flashes to 5 trials for bright flashes. Light-adapted flash ERGs and 30 Hz flicker ERGs were recorded at 3.0 cd.s/m^2 after 10 minutes of adaptation to white 32 cd/m^2 rod suppressing background illumination. ERG a- and b-wave amplitudes from the experimental and control eyes were quantified. Paired *t*-tests were performed using built-in function in MATLAB (v2019; Mathworks, Natick, MA) with the null hypothesis that there are no significant differences between the ERG a- and b-wave amplitudes derived from experimental and control groups.

Histology With Hematoxylin and Eosin and Terminal Deoxynucleotidyl Transferase dUTP Nick end Labeling Staining

After examination by all modalities, the animals were euthanized by sodium pentobarbital overdose (Beuthanasia-D Special 0.22 mg/kg; Intervet Inc., Madison, NJ) intravenously injected into the rabbit marginal ear vein. The globes were harvested and fixed overnight at 4°C in phosphate-buffered saline with 4% paraformaldehyde (pH = 7.4). The specimens were embedded in paraffin and placed in a tissue processor (Tissue-Tek II; Sakura, Tokyo, Japan) for standard paraffin embedding. Histology slides were

prepared at 1 mm distance from each other throughout the globe. Slide preparation started at 12 clock meridian to include the equator of the right eye where the fiber optic bundle was. Eyes were sectioned (6 µm) using a standard paraffin microtome (Shandon AS325; Thermo Scientific, Cheshire, England), and two slides were prepared at each step. For general histology, sections were stained with hematoxylin and eosin (H&E) and photographed with a Leica DM6000 microscope (Leica Microsystems, Wetzlar, Germany). The sections were evaluated for any histopathological disruptions in any ocular layers, especially disorganization and vacuolar appearance in the outer retinal layers (photoreceptor, outer nuclear layer, and retinal pigment epithelium) and loss of cellular stratification on early phase, followed by destruction of the outer nuclear layer and outer segments in late phases, as previously described.[15] The terminal deoxynucleotidyl transferase-mediated deoxyuridine triphosphate nick-end labeling (TUNEL) staining, as previously reported,[16] was performed on the posterior segments of the sections using DeadEnd Colorimetric TUNEL System (Cat. #G3250; Promega Corporation, Madison, WI) according to the manufacturer's instructions.

Results

Wide-Field Fundus Pictures and ICG Angiography Fluorescence Fundus Photography

Wide-field fundus photography in Figure 1, including the area exposed to wide-field laser illumination, demonstrated no fundus or optic disc abnormality.

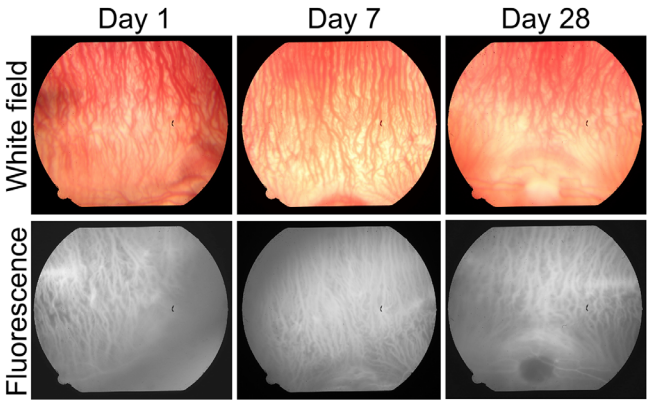

Figure 1. Representative white light fundus photography and ICG angiography fluorescence fundus images of the animals on days 1, 7, and 28 days after laser exposure, showing normal fundus, choroid, and retinal pigment epithelium without any evidence of damage.

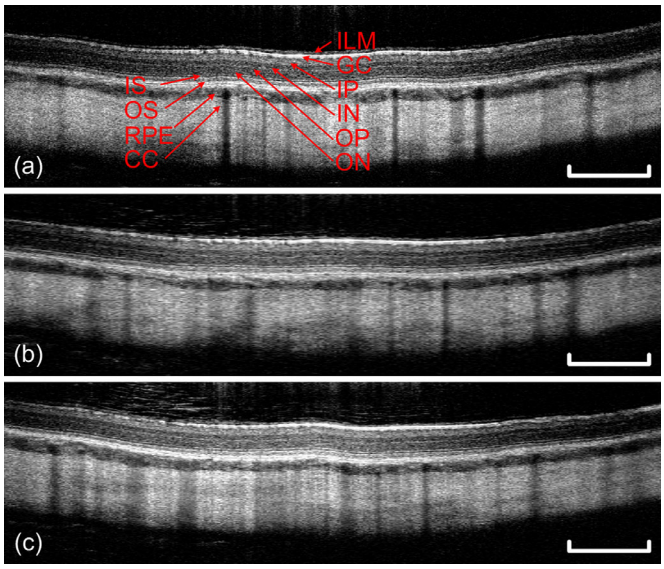

Figure 2. Representative OCT images of the corresponding superior retina of the animals (**A**) 1 day, (**B**) 7 days, and (**C**) 28 days after the laser exposure, showing normal retinal, choroidal, and scleral layers. Scale bars are 500 µm.

There was no retinal vascular or retinal pigment epithelial abnormality. Additionally, fundus ICG angiography fluorescence was also normal with no abnormality in the retinal or choroidal layer or retinal pigment epithelium.

OCT Results

OCT of the corresponding superior quadrant in Figure 2 show that all retinal, retinal pigment epithelium, choroidal, and scleral layers are normal with no evidence of damage.

ERG Analysis

To analyze ERG responses, the rod isolated b-wave was measured from baseline to its peak. For the combined rod-cone response, the negative going a-wave was measured from the baseline to its trough. The b-wave, which reflects bipolar cell activity, was measured from the a-wave trough to the peak of the b-wave. Figure 3 shows the representative ERG waveforms acquired from both the control and experiment eyes.

Averaged quantitative parameters derived from the ERG are shown in Figure 4. There was no significant difference observed in averaged quantitative parameters derived from ERG between the experimental and control eyes at days 1, 7, and 28 ($P > 0.05$).

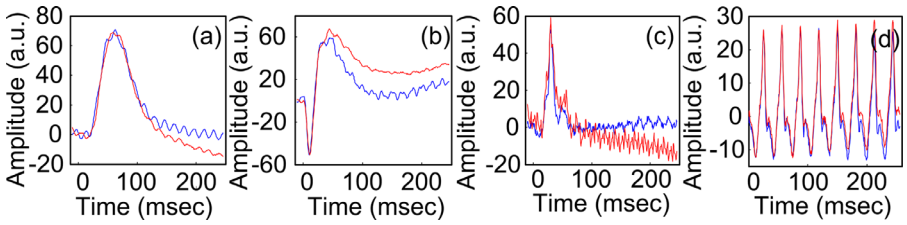

Figure 3. Representative ERG waveforms showing laser exposed eye in red and control eye in blue. Dotted red waveforms are derived from experiment eyes. Solid blue waveforms are derived from control eyes. (**A**) Rod response. (**B**) Combined rod-cone response. (**C**) Light adapted b-wave. (**D**) Light adapted 32 Hz flicker.

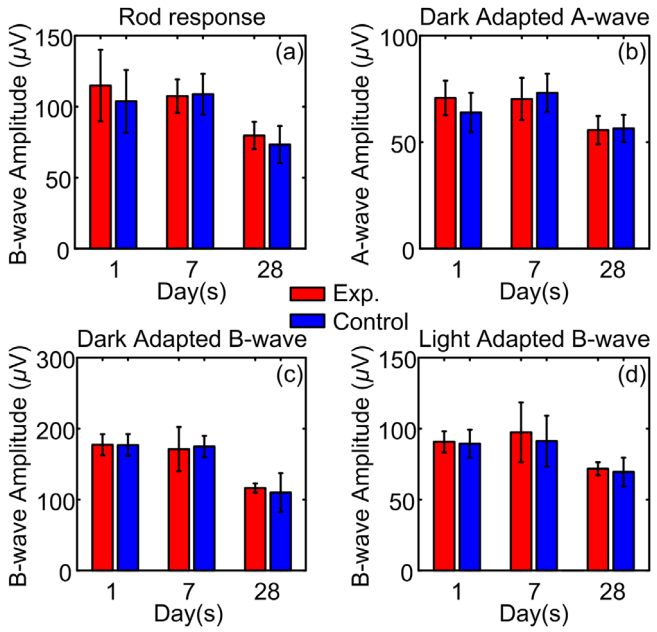

Figure 4. Averaged ERG parameters of experiment and control eyes in days 1, 7, and 28 after the laser exposure, showing no statistical difference between the 2 groups.

Histology of the Sclera

Histology in Figure 5 shows no observable damage to the sclera tissue where the illumination was delivered through the 12 o'clock meridian superiorly at the equator.

We did not observe any histopathological sign of any damage on the sclera where the wide-field laser was applied nor on the rest of the eye.

Histology of Posterior Segment With H&E and TUNEL Staining

No animals had detectable optic nerve toxicity, as shown in Figure 6. The cornea, iris, lens, ciliary body, choroid, and sclera did not appear to be affected in the area where the fiber optic bundle for wide-field laser illumination was applied. Similarly, histopathology did not reveal any disruption in the retinal or choroidal layers in the area where the wide-field laser illumination was delivered or in the remainder of the eyes in any animal.

TUNEL staining to evaluate for any evidence of apoptosis in the eyes are also included in Figure 6. We did not see any sign of apoptosis in the layers of the retina, choroid, and optic nerve.

Discussion

Optical energy in the near infrared range used in PAT of intraocular tumors is nonionizing and nonradiative.[17] The photo-thermal effect is the major cause of possible damage during PAT illumination of the eye. The desirable optical energy level of PAT illumination ranges between (1) an upper limit to avoid photothermal damage to the scleral, retinal, and choroidal tissue, and (2) a lower limit for sufficient penetration through sclera and the intraocular lesion. In our previous study,[1] we showed PAT illumination was enough to pass through the sclera and image the intraocular tumors. In this study, a comprehensive examination of the animal eyes using established modalities of wide-fundus photography, ICG fluorescein angiography, OCT, and histology has shown that the photothermal effect caused by the PAT illumination does not impose any observable damage to the ocular structures, including sclera, choroid, retina, and optic nerve. In addition, the ERG differences between control and experimental eyes shown in Figure 3 are minimal and do not reflect a significant difference in amplitude or implicit time between the two groups. ERG test is a global response of the retina and is not sensitive to small localized areas of damage or to damage in the inner retinal layers. However, with about 70% of the retina exposed to the laser, changes in the ERG response would have been observed if there was

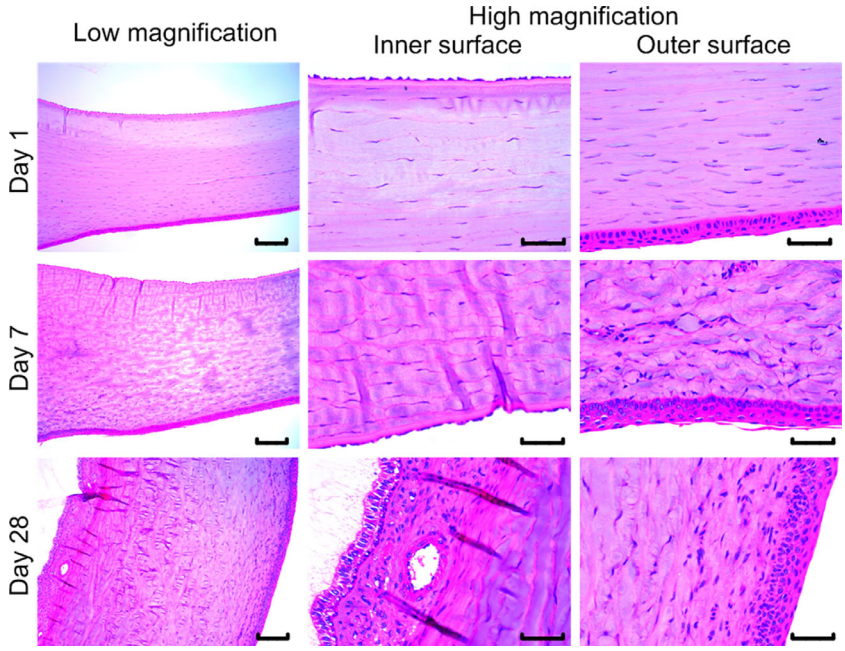

Figure 5. Scleral histology showing no abnormality in the superior quadrant where the wide-field laser illumination was applied. Scale bars in low magnification images are 50 µm. Scale bars in high magnification images are 150 µm.

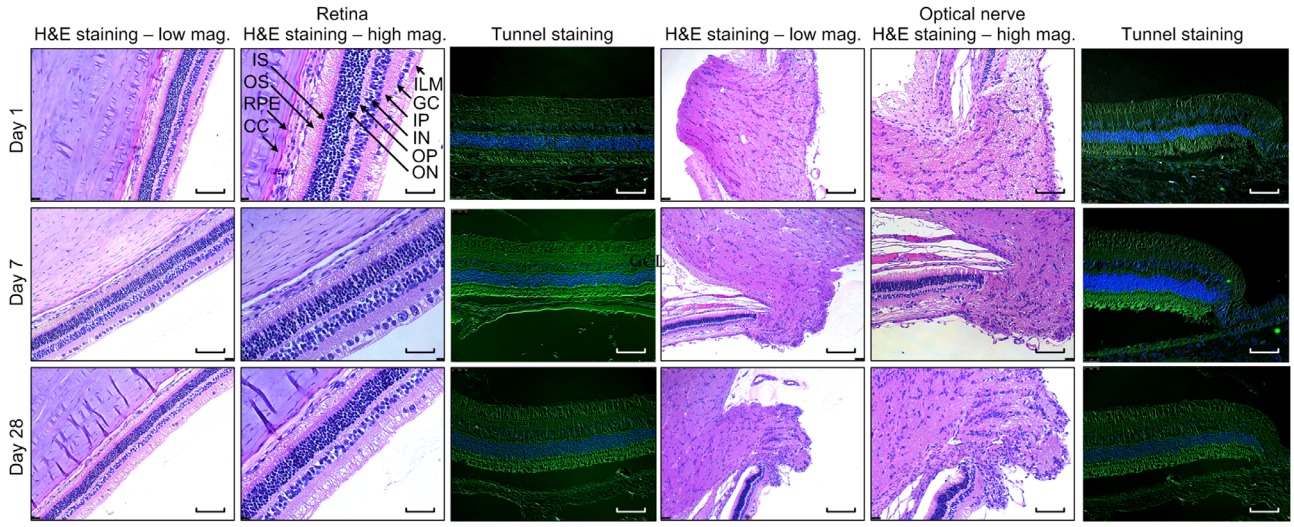

Figure 6. Histopathology and TUNEL staining of the experimental eyes showing normal histopathology of the retinal and choroidal layers and no apoptosis at days 1, 7, and 28. The anatomic layers are labeled. ILM, internal limiting membrane; GCL, ganglion cell layer; IPL, inner plexiform layer; INL, inner nuclear layer; OPL, outer plexiform layer; ONL, outer nuclear layer; IS, inner segment; OS, outer segment; RPE, retinal pigment epithelium; CC, choriocapillaris. Scale bars in the low magnification images are 75 µm. Scale bars in the low magnification images are 30 µm.

significant retinal damage. Results from all the examinations, along with our previous study using enucleated human eyes,[18] support our hypothesis that the optical energy level fits in the safety energy range mentioned above.

Rabbits are selected in this study due to their similarities to human eyes to facilitate clinical translation. As mentioned above, the sclera in rabbits (approximately 200 µm) is substantially thinner than that in humans (approximately 500 µm). The melanin pigment in New Zealand white rabbits is also significantly lower. Therefore, human sclera functions as a better attenuator to optical illumination and protects the retina from photo-thermal damage. Moreover, the larger

dimension of human sclera provides longer path length for spreading the optical energy propagated through the sclera, leading to lower optical density at the retina. Similar difference was observed in studies for semiconductor diode laser in contact transscleral cyclophotocoagulation. In experiments using rabbit eyes, the power of diode laser ranged from 0.6 J to 1.8 J per application.[19] In clinical practice, a higher power of the diode laser was used ranging from 3.5 J to 6 J per application depending on the iris pigmentation and technique.

Conclusion

This study examines the toxicity of laser illumination for ocular PAT. Experimental results derived from live animals show that the energy level used in our previous ex vivo study (i.e. 20 mJ/cm^2), does not impose negative effects to the ocular function and anatomy.

Acknowledgments

The authors thank Chao Tian and Wei Zhang for their help on fundus and OCT imaging. We also thank Yuqing Chen for the generous donation of wild type New Zealand rabbits for the experiments.

Supported by grants R37CA22282901A1, 1R01DK12568701, and 1K08EY027458 (Y.M.P.) by the National Eye Institute. This study is also supported by Richard N and Marilyn K Witham Professorship. This study utilized the Core Center for Vision Research funded by P30 EY007003 from the National Eye Institute.

Disclosure: **G. Xu,** None; **N. Khan,** None; **A. Almazroa,** None; **M. Pawar,** None; **C. Besirli,** None; **Y.M. Paulus,** None; **X. Wang,** None; **H. Demirci,** Castle Bioscience, Advisory board and Aura Bioscience, Investigator

References

1. Xu G, Xue Y, Özkurt ZG, et al. Photoacoustic imaging features of intraocular tumors: Retinoblastoma and uveal melanoma. *PLoS One*. 2017;12:e0170752.
2. Zhu Y, Xu G, Yuan J, et al. Light Emitting Diodes based Photoacoustic Imaging and Potential Clinical Applications. *Sci Rep*. 2018;8:9885.
3. Tian C, Zhang W, Mordovanakis A, Wang X, Paulus YM. Noninvasive chorioretinal imaging in living rabbits using integrated photoacoustic microscopy and optical coherence tomography. *Opt Express*. 2017;25:15947–15955.
4. de la Zerda A, Paulus YM, Teed R, et al. Photoacoustic ocular imaging. *Opt Lett*. 2010;35:270–272.
5. Li Y, Zhang W, Nguyen VP, et al. Retinal safety evaluation of photoacoustic microscopy. *Exp Eye Res*. 2021;202:108368.
6. Yuan J, Xu G, Yu Y, et al. Real-time photoacoustic and ultrasound dual-modality imaging system facilitated with graphics processing unit and code parallel optimization. *J Biomed Opt*. 2013;18:86001–86001.
7. Lund BJ, Lund DJ, Edsall PR. Damage Threshold from Large Retinal Spot Size Repetitive-pulse Laser Exposures. *Health Physics*. 2014;107:292–299.
8. Yumita A, Shirato S, Kitazawa Y. Retinal damage threshold of ophthalmic Q-switched Nd-YAG laser in monkey eyes. *Jpn J Ophthalmol*. 1986;30:100–115.
9. Vogel A, Dlugos C, Nuffer R, Birngruber R. Optical properties of human sclera, and their consequences for transscleral laser applications. *Lasers Surg Med*. 1991;11:331–340.
10. Smith RS, Stein MN. Ocular Hazards of Transscleral Laser Radiation: I. Spectral reflection and transmission of the sclera, choroid and retina. *Am J Ophthalmol*. 1968;66:21–31.
11. Bashkatov AN, Genina EA, Kochubey VI, Tuchin VV. Optical properties of human sclera in spectral range 370–2500 nm. *Opt Spectroscopy*. 2010;109:197–204.
12. International Electrotechnical Commission. *Photobiological safety of lamps and lamp systems*. Geneva, Switzerland: International Electrotechnical Commission; 2006.
13. Hughes A. A schematic eye for the rabbit. *Vis Res*. 1972;12:123–IN126.
14. Reichenbach A, Schnitzer J, Friedrich A, Ziegert W, Brückner G, Schober W. Development of the rabbit retina. *Anatomy Embryol*. 1991;183:287–297.
15. Wood JPM, Shibeeb OS, Plunkett M, Casson RJ, Chidlow G. Retinal Damage Profiles and Neuronal Effects of Laser Treatment: Comparison of a Conventional Photocoagulator and a Novel 3-Nanosecond Pulse Laser. *Invest Ophthalmol Vis Sci*. 2013;54:2305–2318.

16. Pawar M, Busov B, Chandrasekhar A, Yao J, Zacks DN, Besirli CG. FAS apoptotic inhibitory molecule 2 is a stress-induced intrinsic neuroprotective factor in the retina. *Cell Death Differentiation*. 2017;24:1799–1810.
17. Yodh A, Chance B. Spectroscopy and imaging with diffusing light. *Physics Today*. 1995;48:34.
18. Duerr ERH, Sayed MS, Moster SJ, et al. Transscleral Diode Laser Cyclophotocoagulation: A Comparison of Slow Coagulation and Standard Coagulation Techniques. *Ophthalmology Glaucoma*. 2018;1:115–122.
19. Schuman JS, Jacobson JJ, Puliafito CA, Noecker RJ, Reidy WT. Experimental Use of Semiconductor Diode Laser in Contact Transscleral Cyclophotocoagulation in Rabbits. *Arch Ophthalmol*. 1990;108:1152–1157.